

INFLUENCE OF CHROMATIC DISPERSION, DISPERSION SLOPE, DISPERSION CURVATURE ON MICROWAVE GENERATION USING TWO CASCADE MODULATORS

Mandeep Singh¹ and S.K. Raghuwanshi²

Photonics Research Laboratory, Department of Electronics Engineering, Indian School of Mines, India

E-mail: ¹mandeepsingh@ismu.ac.in and ²sanjeevrus@yahoo.com

Abstract

This work presents a theoretical study of harmonic generation of microwave signals after detection of a modulated optical carrier in cascaded two electro-optic modulators. Dispersion is one of the major limiting factors for microwave generation in microwave photonics. In this paper, we analyze influence of chromatic dispersion, dispersion slope, dispersion curvature on microwave generation using two cascaded MZMs and it has been found that output intensity of photodetector reduces when dispersion term up to fifth order are added. We have used the two cascaded Mach-Zehnder Modulators for our proposed model and tried to show the dispersion effect with the help of modulation depth factor of MZM, which have been not discussed earlier.

Keywords:

Dispersion Slope, Dispersion Curvature, Fiber Bragg Grating, Microwave Photonics, Mach-Zehnder Modulator

1. INTRODUCTION

Microwave Photonics (MWP) is the study of devices at microwave frequency and their application to the optical devices [1-3]. Research in the field of microwave photonics is going on in a rapid phase. Various application of MWP includes like radar, communication system, sensor network, warfare systems [4]. Main advantages of MWP technology over conventional electrical-transmission technology include reduced size, weight and cost, low and constant attenuation over the entire microwave and millimeter-wave modulation frequency range, immunity to electromagnetic interference, low dispersion, no electro-optical conversions and high data-transfer capacity [5]. In the past few months various methods have been proposed for microwave / millimeter wave signal generation but simple method is beating of optical carriers from two laser sources at THz frequency, followed by photodiode (PD) [6-7]. But its disadvantage is that high phase noise is produce if phase of two beating optical carriers are not correlated [6]. Other advance methods include

optical injection locking [8-9] and optical phase – locked loop (OPLL) [10-11]. But problem with this method is that optical sources with very narrow linewidth mainly in KHz are required [12]. Solution to this problem is that we can use Lithium-niobate Mach-Zehnder Modulator ($LiNbO_3$ – MZM), which involves concept of frequency multiplication [6]. O’Reilly et al proposed a method to generate microwave / millimeter wave using MZM [13]. Mach-Zehnder Modulator (MZM) can be operated in two transmission points: Maximum Transmission Point (MAXTP) and Minimum Transmission Point (MINTP) [14].

Dispersion is one of the most important limiting factors in MWP. Dispersion is spreading out of light pulses as they travel along a fibre and mainly occur due to the dependence of speed of light through the fibre on the wavelength [6]. Unlike attenuation, dispersion does not weak a signal. It only blurs the optical signal transmitted through optical fibre. In this paper, we analyze the effect of higher order dispersion term, i.e. up to fifth order, dispersion parameters on microwave/ millimeter wave generation using two cascaded MZMs.

Section 2 consists of the theory of proposed model for millimeter wave / microwave generation, followed by the derivation of output of two MZM in series with higher order dispersion terms. In section 3 we plotted various graphs of output intensity of photo detector versus modulation depth (β) considering individual dispersion term and combinations of dispersion term up to fifth order.

2. PROPOSED MODEL

A novel approach to generate microwave wave using two series MZMs is shown in Fig.1. An optical carrier of 193.1 THz and an electrical drive signal of frequency 12.5 GHz are applied to a first Mach-Zehnder Modulator (MZM). We have used ITU’s G.653 fiber of different length for calculation and simulation.

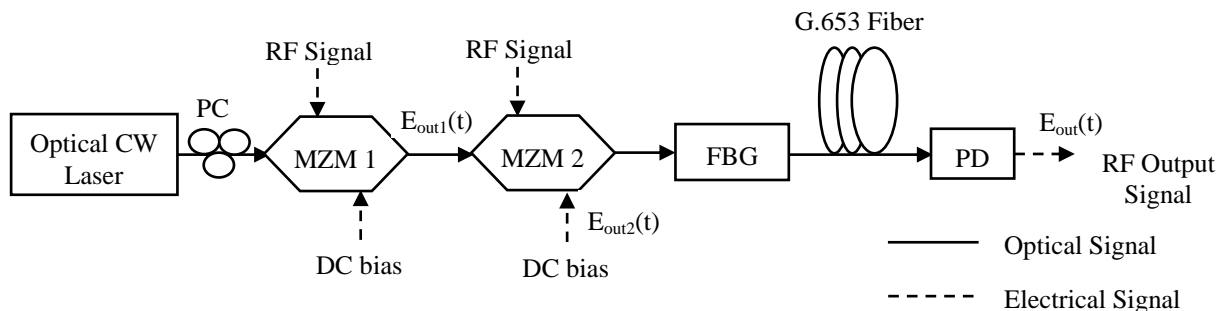


Fig.1. Generalized diagram of millimeter wave / microwave frequency generation system using two series MZMs. CW: continuous wave, PC: Polarization controller, MZM: Mach-Zehnder modulator, FBG: Fibre Bragg Grating, G.653: International Telecommunication Union’s standardized, PD: Photo Detector

Consider the case when only one arm of first MZM is modulated, the phase difference becomes [6],

$$\Delta\phi = \frac{\Delta n \cdot 2\pi \cdot L}{\lambda} \quad (1)$$

where, Δn is the optical refractive index change in the arm of modulator, λ is optical wavelength, L is the length of the modulating arm of MZM. Due to Pockel's effect in $LiNbO_3$ MZM, Eq.(1) becomes [6],

$$\Delta\phi = \frac{n_0^3 \cdot r_{ij} \cdot V_{RF} \cdot 2\pi \cdot L}{2 \cdot d \cdot \lambda}$$

where, r_{ij} is the electro-optic coefficient of $LiNbO_3$ crystal, V_{RF} is the amplitude of applied low frequency RF signal, d is the distance between MZM arms.

As, $V_\pi = \frac{d \cdot \pi}{n_0^3 \cdot r_{ij} \cdot L}$, therefore above equation reduces to,

$$\Delta\phi = \frac{V_{RF} \cdot \pi}{V_\pi}$$

where, V_π is the voltage value at which voltage induced phase difference reaches 180° .

If the MZM is driven by a low frequency electrical signal and biased with a constant DC voltage then phase difference becomes [6],

$$\Delta\phi[V(t)] = \phi_0 + \frac{V_{RF} \cdot \pi}{V_\pi} \quad (2)$$

where, $\Delta\phi[V(t)]$ is the optical phase difference caused by between the two arms of the MZM, ϕ_0 is a constant phase shift, E_{RF} is the amplitude of the electrical drive signal. If the MZM is driven by a sinusoidal electrical signal and biased with a constant dc voltage, $\phi[V(t)]$, then electric field at the output of a lithium niobate MZM can be approximately expressed by [6],

$$E_{out1}(t) = E_{in}(t) \cdot \cos\left[\frac{\phi[V(t)]}{2}\right]$$

or

$$E_{out1}(t) = E_0(t) \cdot \cos\left[\frac{\phi[V(t)]}{2}\right] \cdot \cos(\omega_0 t) \quad (3)$$

where, $E_0(t)$ and ω_0 are, respectively, the electric field amplitude and the angular frequency of the input optical carrier, $V(t)$ is the applied RF electrical drive voltage. The generalized electric field equation at the output of modulator up to n terms can be written using Eq.(3) and Eq.(4), as follows [14]:

$$\begin{aligned} E(t) = & E_0 \cos(\Phi/2) \left\{ \cos(\omega_0 t + \Phi/2) J_0(\beta) + \right. \\ & \sum_{n=1}^{\infty} (-1)^n J_{2n}(\beta) \left[\cos(\omega_0 t + 2n(\omega_{RF} t + \phi) + \Phi/2) + \right. \\ & \left. \left. \cos(\omega_0 t - 2n(\omega_{RF} t + \phi) + \Phi/2) \right] \right\} + \\ & E_0 \sin(\Phi/2) \left\{ \sum_{n=1}^{\infty} (-1)^n J_{2n-1}(\beta) \left[\cos(\omega_0 t + (2n-1) \right. \right. \\ & \left. \left. \times (\omega_{RF} t + \phi) + \Phi/2) + \cos(\omega_0 t - (2n-1)(\omega_{RF} t + \phi) + \Phi/2) \right] \right\} \end{aligned} \quad (4)$$

where, $\beta = \frac{V_{RF}}{V_\pi} \cdot \frac{\pi}{2}$ is a modulation depth, Φ is the phase

difference between the arms of the modulator and ϕ is the phase of the electrical drive RF signal. The MZM can be operated at either Maximum transmission point (MAXTP), i.e. $\Phi = 0$ or Minimum transmission point (MINTP), i.e. $\Phi = \pi$ [14]. Hence, by connecting two MZMs in series we get four combinations: 1) MAXTP, MAXTP; 2) MAXTP, MINTP; 3) MINTP, MAXTP; 4) MINTP, MINTP. An FBG (Fiber Bragg Grating) is connected at the output of the MZM to remove the optical carrier and hence act as optical filter.

2.1 MAXTP, MAXTP

As both MZMs are operating at MAXTP. Therefore, $\Phi = 0$ for both MZMs. Expanding Eq.(4) for $n = 2$, the electric field ($E_{out1}(t)$) at the output of first MZM is given by,

$$\begin{aligned} E_{out1}(t) = & E_0 \left\{ J_0(\beta_1) \cdot \cos(\omega_0 t) \right. \\ & - J_2(\beta_1) \cos(\omega_0 t - 2\omega_{RF} t - 2\phi_1) \\ & \left. - J_2(\beta_1) \cos(\omega_0 t + 2\omega_{RF} t + 2\phi_1) \right\} \end{aligned} \quad (5)$$

where, ϕ_1 is the initial phase of an electrical drive signal for MZM1 and β_1 is the modulation depth of MZM1. If the attenuation of the Fiber Bragg Grating at its center notch wavelength is α dB. The electric field at the output of FBG becomes,

$$\begin{aligned} E_{out1}(t) = & E_0 \left\{ k J_0(\beta_1) \cdot \cos(\omega_0 t) \right. \\ & - J_2(\beta_1) \cos(\omega_0 t - 2\omega_{RF} t - 2\phi_1) \\ & \left. - J_2(\beta_1) \cos(\omega_0 t + 2\omega_{RF} t + 2\phi_1) \right\} \end{aligned} \quad (6)$$

where, k is the electrical field attenuation factor and related to α by $\alpha = -20 \log_{10} k$.

As shown in Fig.1, $E_{out1}(t)$ is input to the second MZM. Therefore, electric field ($E_{out2}(t)$) output of second modulator is given by,

$$\begin{aligned} E_{out2}(t) = & E_0 \left\{ J_2(\beta_1) \cdot J_2(\beta_2) \cos(\omega_0 t - 4\omega_{RF} t - 2\phi_1 - 2\phi_2) \right. \\ & - k J_2(\beta_1) \cdot J_0(\beta_2) \cos(\omega_0 t - 2\omega_{RF} t - 2\phi_1) \\ & - J_0(\beta_1) \cdot J_2(\beta_2) \cos(\omega_0 t - 2\omega_{RF} t - 2\phi_2) \\ & + J_2(\beta_1) \cdot J_2(\beta_2) \cos(\omega_0 t - 2\phi_1 + 2\phi_2) \\ & + k J_0(\beta_1) \cdot J_0(\beta_2) \cos(\omega_0 t) \\ & + J_2(\beta_1) \cdot J_2(\beta_2) \cos(\omega_0 t + 2\phi_1 + 2\phi_2) \\ & - J_0(\beta_1) \cdot J_2(\beta_2) \cos(\omega_0 t + 2\omega_{RF} t + 2\phi_2) \\ & - k J_2(\beta_1) \cdot J_0(\beta_2) \cos(\omega_0 t + 2\omega_{RF} t + 2\phi_1) \\ & \left. + J_2(\beta_1) \cdot J_2(\beta_2) \cos(\omega_0 t + 4\omega_{RF} t + 2\phi_1 + 2\phi_2) \right\} \end{aligned} \quad (7)$$

where, ϕ_1 & ϕ_2 are the initial phases of the applied RF electrical drive signal of MZM1 and MZM2, respectively and β_1 & β_2 are the modulation depth of the MZM1 and MZM2, respectively. Considering initial phases of applied RF electrical drive signal for both the MZMs equal to zero, i.e. $\phi_1 = \phi_2 = 0$.

$$E_{out2}(t) = E_0 \left\{ \left[k J_0(\beta_1) J_0(\beta_2) + 2 J_2(\beta_1) J_2(\beta_2) \right] \cos(\omega_0 t) \right. \\ \left. - \left[k J_2(\beta_1) J_0(\beta_2) + J_0(\beta_1) J_2(\beta_2) \right] \left[\begin{array}{l} \cos(\omega_0 t - 2\omega_{RF} t) + \\ \cos(\omega_0 t + 2\omega_{RF} t) \end{array} \right] \right. \\ \left. + J_2(\beta_1) J_2(\beta_2) \left[\begin{array}{l} \cos(\omega_0 t - 4\omega_{RF} t) + \\ \cos(\omega_0 t + 4\omega_{RF} t) \end{array} \right] \right\} \quad (8)$$

The electric field representing the optical signal at the end of the transmission over a ITU G.653 fiber can be obtained by adding the transmission phase delay $[\beta(\omega_0 \pm 2n\omega_{RF})L]$ to the corresponding optical sideband shown in Eq.(8).

$$E_{out2}(t) = E_0 \left\{ \left[\begin{array}{l} k J_0(\beta_1) J_0(\beta_2) + \\ 2 J_2(\beta_1) J_2(\beta_2) \end{array} \right] \cos(\omega_0 t + \beta(\omega_0)L) \right. \\ \left. - \left[\begin{array}{l} k J_2(\beta_1) J_0(\beta_2) + \\ J_0(\beta_1) J_2(\beta_2) \end{array} \right] \left[\begin{array}{l} (\omega_0 t - 2\omega_{RF} t) + \\ \beta(\omega_0 - 2\omega_{RF})L \end{array} \right] \right. \\ \left. + \cos(\omega_0 t + 2\omega_{RF} t + \beta(\omega_0 + 2\omega_{RF})L) \right. \\ \left. + J_2(\beta_1) J_2(\beta_2) \left[\begin{array}{l} (\omega_0 t - 4\omega_{RF} t) + \\ \beta(\omega_0 - 4\omega_{RF})L \end{array} \right] \right. \\ \left. + \cos(\omega_0 t + 4\omega_{RF} t + \beta(\omega_0 + 4\omega_{RF})L) \right\} \quad (9)$$

Expanding the propagation constant $\beta(\omega)$ of the fiber for each optical sideband using Taylor's series around the angular frequency of the optical carrier [15].

$$\beta(\omega_0 \pm 2n\omega_{RF}) = \beta(\omega_0) + \frac{d\beta}{d\omega}(\pm 2n\omega_{RF}) + \frac{1}{2} \frac{d^2\beta}{d\omega^2}(\pm 2n\omega_{RF})^2 \\ + \frac{1}{6} \frac{d^3\beta}{d\omega^3}(\pm 2n\omega_{RF})^3 + \frac{1}{24} \frac{d^4\beta}{d\omega^4}(\pm 2n\omega_{RF})^4 + \frac{1}{120} \frac{d^5\beta}{d\omega^5}(\pm 2n\omega_{RF})^5 \dots \\ \beta(\omega_0 \pm 2n\omega_{RF}) = \beta(\omega_0) + \beta^1(\omega_0)(\pm 2n\omega_{RF}) + \\ \frac{1}{2} \beta^2(\omega_0)(\pm 2n\omega_{RF})^2 + \frac{1}{6} \beta^3(\omega_0)(\pm 2n\omega_{RF})^3 + \\ \frac{1}{24} \beta^4(\omega_0)(\pm 2n\omega_{RF})^4 + \frac{1}{120} \beta^5(\omega_0)(\pm 2n\omega_{RF})^5 \dots \quad (10)$$

where, $\beta^1(\omega_0) = d\beta/d\omega = \tau$, the propagation delay per optical length.

The second-order dispersion parameter is given by [15],

$$\beta^2(\omega_0) = \frac{d\tau}{d\omega} = \frac{\lambda^2}{2\pi c} \frac{\partial \tau}{\partial \lambda} = \frac{\lambda^2}{2\pi c} D \quad (11)$$

where, D is the Group Velocity Dispersion (GVD).

The third-order dispersion parameter or Dispersion Slope is given by [15],

$$\beta^3(\omega_0) = \frac{d^2\tau}{d\omega^2} = \frac{\lambda^2}{(2\pi c)^2} \left[\lambda^2 \frac{\partial^2 \tau}{\partial \lambda^2} + 2\lambda \frac{\partial \tau}{\partial \lambda} \right] \\ = \frac{\lambda^2}{(2\pi c)^2} \left[\lambda^2 D_1 + 2\lambda D \right] \quad (12)$$

where, $(D_1 = S)$ is the Dispersion Slope.

The fourth-order dispersion parameter or Dispersion curvature is given by [15],

$$\beta^4(\omega_0) = \frac{d^3\tau}{d\omega^3} = \frac{\lambda^3}{(2\pi c)^3} \left[\lambda^3 \frac{\partial^3 \tau}{\partial \lambda^3} + 6\lambda^2 \frac{\partial^2 \tau}{\partial \lambda^2} + 6\lambda \frac{\partial \tau}{\partial \lambda} \right] \\ = \frac{\lambda^3}{(2\pi c)^3} \left[\lambda^3 D_2 + 6\lambda^2 D_1 + 6\lambda D \right] \quad (13)$$

The fifth-order dispersion parameter or Dispersion curvature is given by [15],

$$\beta^5(\omega_0) = \frac{d^4\tau}{d\omega^4} = \\ \frac{\lambda^4}{(2\pi c)^4} \left[\lambda^4 \frac{\partial^4 \tau}{\partial \lambda^4} + 12\lambda^3 \frac{\partial^3 \tau}{\partial \lambda^3} + 36\lambda^2 \frac{\partial^2 \tau}{\partial \lambda^2} + 24\lambda \frac{\partial \tau}{\partial \lambda} \right] \\ = \frac{\lambda^4}{(2\pi c)^4} \left[\lambda^4 D_3 + 12\lambda^3 D_2 + 36\lambda^2 D_1 + 24\lambda D \right] \quad (14)$$

where, $\frac{d\tau}{d\lambda} = D$, $\frac{d^2\tau}{d\lambda^2} = D_1$, $\frac{d^3\tau}{d\lambda^3} = D_2$, $\frac{d^4\tau}{d\lambda^4} = D_3$. We have

neglected the dispersion parameter $\beta^1(\omega_0) = d\beta/d\omega = \tau$, because it produces only a phase delay of the carrier signal and has no influence on distortion of the signal. Inserting dispersion parameter in Eq.(9) up to fifth order with the help of Eq.(10), Eq.(11), Eq.(12), Eq.(13) and Eq.(14) i.e. the electric field at the output of MZM2 with dispersion is given by,

$$E_{out2}(t) = E_0 \left\{ \left[\begin{array}{l} k J_0(\beta_1) J_0(\beta_2) + \\ 2 J_2(\beta_1) J_2(\beta_2) \end{array} \right] \cos(\omega_0 t + \beta(\omega_0)L) \right. \\ \left. - 2 \cdot \left[\begin{array}{l} k J_2(\beta_1) J_0(\beta_2) + \\ J_0(\beta_1) J_2(\beta_2) \end{array} \right] \right. \\ \left. \times \cos \left[\begin{array}{l} \omega_0 t + \beta(\omega_0)L + \frac{1}{2} \beta^2(\omega_0)(2\omega_{RF})^2 L \\ + \frac{1}{24} \beta^4(\omega_0)(2\omega_{RF})^4 L \end{array} \right] \right. \\ \left. \times \cos \left[\begin{array}{l} 2\omega_{RF} t + \beta^1(\omega_0)(2\omega_{RF})L + \frac{1}{6} \beta^3(\omega_0)(2\omega_{RF})^3 L \\ + \frac{1}{120} \beta^5(\omega_0)(2\omega_{RF})^5 L \end{array} \right] \right. \\ \left. + 2 J_2(\beta_1) J_2(\beta_2) \times \cos \left[\begin{array}{l} \omega_0 t + \beta(\omega_0)L + \frac{1}{2} \beta^2(\omega_0)(4\omega_{RF})^2 L + \\ \frac{1}{24} \beta^4(\omega_0)(4\omega_{RF})^4 L \end{array} \right] \right. \\ \left. \times \cos \left[\begin{array}{l} 4\omega_{RF} t + \beta^1(\omega_0)(4\omega_{RF})L + \frac{1}{6} \beta^3(\omega_0)(4\omega_{RF})^3 L \\ + \frac{1}{120} \beta^5(\omega_0)(4\omega_{RF})^5 L \end{array} \right] \right\}$$

At the end of the fiber, $z = L$, the output intensity of photo detector is given by,

$$I_{PD}(t) = E_{out2} \cdot E_{out2}^* \quad (15)$$

2.2 MINTP, MINTP

As both MZMs are operating at MINTP. Therefore, $\Phi = \pi$ for both MZMs. Expanding Eq.(4) for $n = 2$, the electric field ($E_{out1}(t)$) at the output of first MZM is given by,

$$E_{out1}(t) = E_0 \left\{ \begin{aligned} & \left[J_1(\beta_1) \sin((\omega_0 - \omega_{RF})t - \phi_1) + \right. \\ & \left. J_1(\beta_1) \sin(\omega_0 t + \omega_{RF}t + \phi_1) \right] \\ & - \left[J_3(\beta_1) \sin((\omega_0 - 3\omega_{RF})t - 3\phi_1) + \right. \\ & \left. J_3(\beta_1) \sin(\omega_0 t + 3\omega_{RF}t + 3\phi_1) \right] \end{aligned} \right\}$$

where, ϕ_1 is the initial phase of the electrical drive signal for MZM1 and β_1 is the modulation depth of MZM1. As shown in Fig.1, $E_{out1}(t)$ is input to the MZM2. Therefore, electric field ($E_{out2}(t)$) output of MZM2 is given by,

$$E_{out2}(t) = E_0 \{ J_1(\beta_1) J_1(\beta_2) \cos(\omega_0 t - 2\omega_{RF}t - \phi_1 - \phi_2) + J_1(\beta_1) J_1(\beta_2) \cos(\omega_0 t - \phi_1 + \phi_2) - J_1(\beta_1) J_3(\beta_2) \cos(\omega_0 t - 4\omega_{RF}t - \phi_1 - 3\phi_2) - J_1(\beta_1) J_3(\beta_2) \cos(\omega_0 t + 2\omega_{RF}t - \phi_1 + 3\phi_2) + J_1(\beta_1) J_1(\beta_2) \cos(\omega_0 t + \phi_1 - \phi_2) + J_1(\beta_1) J_1(\beta_2) \cos(\omega_0 t + 2\omega_{RF}t + \phi_1 + \phi_2) - J_1(\beta_1) J_3(\beta_2) \cos(\omega_0 t - 2\omega_{RF}t + \phi_1 - 3\phi_2) - J_1(\beta_1) J_3(\beta_2) \cos(\omega_0 t + 4\omega_{RF}t + \phi_1 + 3\phi_2) - J_3(\beta_1) J_1(\beta_2) \cos(\omega_0 t - 4\omega_{RF}t - 3\phi_1 - \phi_2) - J_3(\beta_1) J_1(\beta_2) \cos(\omega_0 t - 2\omega_{RF}t - 3\phi_1 + \phi_2) + J_3(\beta_1) J_3(\beta_2) \cos(\omega_0 t - 6\omega_{RF}t - 3\phi_1 - 3\phi_2) + J_3(\beta_1) J_3(\beta_2) \cos(\omega_0 t - 3\phi_1 + 3\phi_2) - J_3(\beta_1) J_1(\beta_2) \cos(\omega_0 t + 2\omega_{RF}t + 3\phi_1 - \phi_2) - J_3(\beta_1) J_1(\beta_2) \cos(\omega_0 t + 4\omega_{RF}t + 3\phi_1 + \phi_2) + J_3(\beta_1) J_3(\beta_2) \cos(\omega_0 t + 3\phi_1 - 3\phi_2) + J_3(\beta_1) J_3(\beta_2) \cos(\omega_0 t + 6\omega_{RF}t + 3\phi_1 + 3\phi_2) \}$$
 (16)

where, ϕ_1 & ϕ_2 are the initial phases of the applied RF electrical drive signal of MZM1 and MZM2, respectively and β_1 & β_2 are the modulation depth of the MZM1 and MZM2, respectively.

Considering initial phases of applied RF electrical drive signal for both the MZMs equal to zero, i.e. $\phi_1 = \phi_2 = 0$.

$$E_{out2}(t) = E_0 \left\{ \begin{aligned} & \left[\frac{2J_1(\beta_1)J_1(\beta_2) +}{2J_3(\beta_1)J_3(\beta_2)} \right] \cos(\omega_0 t) \\ & + [J_1(\beta_1)J_1(\beta_2) - J_1(\beta_1)J_3(\beta_2) - J_3(\beta_1)J_3(\beta_1)] \\ & \times [\cos(\omega_0 t - 2\omega_{RF}t) + \cos(\omega_0 t + 2\omega_{RF}t)] \\ & - [J_1(\beta_1)J_3(\beta_2) + J_3(\beta_1)J_1(\beta_2)] \\ & \times [\cos(\omega_0 t - 4\omega_{RF}t) + \cos(\omega_0 t + 4\omega_{RF}t)] \\ & + J_3(\beta_1)J_3(\beta_2) \left[\frac{\cos(\omega_0 t - 6\omega_{RF}t) +}{\cos(\omega_0 t + 6\omega_{RF}t)} \right] \end{aligned} \right\}$$
 (17)

The electric field representing the optical signal at the end of the transmission over an ITU G.653 Non Zero Dispersion Shifted fibre (NZDSF) can be obtained by adding the transmission phase delay $[\beta(\omega_0 \pm 2n\omega_{RF})L]$ to the corresponding optical sideband shown in Eq.(17).

$$E_{out2}(t) = E_0 \left\{ \begin{aligned} & \left[\frac{2J_1(\beta_1)J_1(\beta_2) +}{2J_3(\beta_1)J_3(\beta_2)} \right] \cos(\omega_0 t + \beta(\omega_0)L) \\ & + \left[\frac{J_1(\beta_1)J_1(\beta_2) - J_1(\beta_1)J_3(\beta_2) -}{J_3(\beta_1)J_3(\beta_1)} \right] \\ & \times \left[\frac{\cos(\omega_0 t - 2\omega_{RF}t + \beta(\omega_0 - 2\omega_{RF})L) +}{\cos(\omega_0 t + 2\omega_{RF}t + \beta(\omega_0 + 2\omega_{RF})L)} \right] \\ & - [J_1(\beta_1)J_3(\beta_2) + J_3(\beta_1)J_1(\beta_2)] \\ & \times \left[\frac{\cos(\omega_0 t - 4\omega_{RF}t + \beta(\omega_0 - 4\omega_{RF})L) +}{\cos(\omega_0 t + 4\omega_{RF}t + \beta(\omega_0 + 4\omega_{RF})L)} \right] \\ & + J_3(\beta_1)J_3(\beta_2) \left[\frac{\cos(\omega_0 t - 6\omega_{RF}t + \beta(\omega_0 - 6\omega_{RF})L) +}{\cos(\omega_0 t + 6\omega_{RF}t + \beta(\omega_0 + 6\omega_{RF})L)} \right] \end{aligned} \right\}$$
 (18)

Inserting dispersion parameter in Eq.(18) up to fifth order with the help of Eq.(10), Eq.(11), Eq.(12), Eq.(13) and Eq.(14) i.e. the electric field at the output of MZM2 with dispersion is given by,

$$E_{out2}(t) = E_0 \left\{ \begin{aligned} & \left[\frac{2J_1(\beta_1)J_1(\beta_2) +}{2J_3(\beta_1)J_3(\beta_2)} \right] \cos(\omega_0 t + \beta(\omega_0)L) \\ & + 2 \left[\frac{J_1(\beta_1)J_1(\beta_2) - J_1(\beta_1)J_3(\beta_2) -}{J_3(\beta_1)J_3(\beta_1)} \right] \\ & \times \cos \left(\omega_0 t + \beta(\omega_0)L + \frac{1}{2} \beta^2(\omega_0)(2\omega_{RF})^3 L + \frac{1}{24} \beta^4(\omega_0)(2\omega_{RF})^4 L \right) \\ & \cos \left(\frac{2\omega_{RF}t + \beta(\omega_0)(2\omega_{RF}L) + \frac{1}{6} \beta^3(\omega_0)(2\omega_{RF})^3 L +}{\frac{1}{120} \beta^5(\omega_0)(2\omega_{RF})^5 L} \right) \\ & - [J_1(\beta_1)J_3(\beta_2) + J_3(\beta_1)J_1(\beta_2)] \\ & \times \cos \left(\omega_0 t + \beta(\omega_0)L + \frac{1}{2} \beta^2(\omega_0)(4\omega_{RF})^2 L + \frac{1}{24} \beta^4(\omega_0)(4\omega_{RF})^4 L \right) \\ & \times \cos \left(\frac{4\omega_{RF}t + \beta(\omega_0)(4\omega_{RF}L) + \frac{1}{6} \beta^3(\omega_0)(4\omega_{RF})^3 L +}{\frac{1}{120} \beta^5(\omega_0)(4\omega_{RF})^5 L} \right) \\ & + J_3(\beta_1)J_3(\beta_2) \times \cos \left(\omega_0 t + \beta(\omega_0)L + \frac{1}{2} \beta^2(\omega_0)(6\omega_{RF})^2 L + \frac{1}{24} \beta^4(\omega_0)(6\omega_{RF})^4 L \right) \\ & \times \cos \left(\frac{6\omega_{RF}t + \beta(\omega_0)(6\omega_{RF}L) + \frac{1}{6} \beta^3(\omega_0)(6\omega_{RF})^3 L +}{\frac{1}{120} \beta^5(\omega_0)(6\omega_{RF})^5 L} \right) \end{aligned} \right\}$$
 (19)

At the end of the fiber, $z = L$, the output intensity of photo detector is given by,

$$I_{PD}(t) = E_{out2} \cdot E_{out2}^*$$

2.3 MINTP, MAXTP

As the MZM1 is biased at the MINTP and MZM2 is biased at MAXTP. Therefore, $\Phi_1 = \pi$ and $\Phi_2 = 0$ for MZM1 and MZM2, respectively. Expanding Eq.(4) for $n = 2$, the electric field ($E_{out1}(t)$) at the output of MZM1 is given by,

$$E_{out1}(t) = E_0 \left\{ \begin{aligned} & \left[\begin{aligned} & J_1(\beta_1) \sin((\omega_0 - \omega_{RF})t - \phi_1) + \\ & J_1(\beta_1) \sin(\omega_0 t + \omega_{RF} t + \phi_1) \end{aligned} \right] \\ & - \left[\begin{aligned} & J_3(\beta_1) \sin((\omega_0 - 3\omega_{RF})t - 3\phi_1) + \\ & J_3(\beta_1) \sin(\omega_0 t + 3\omega_{RF} t + 3\phi_1) \end{aligned} \right] \end{aligned} \right\} \quad (20)$$

where, ϕ_1 is the initial phase of the electrical drive signal for MZM1 and β_1 is the modulation depth of MZM1. As shown in Fig.1, $E_{out1}(t)$ is input to the MZM2. Therefore, electric field ($E_{out2}(t)$) output of MZM2 is given by,

$$E_{out2}(t) = E_0 \left\{ \begin{aligned} & \left[\begin{aligned} & J_1(\beta_1) J_2(\beta_2) - \\ & k J_1(\beta_1) J_0(\beta_2) \end{aligned} \right] \\ & \times \left[\sin(\omega_0 t - \omega_{RF} t) + \sin(\omega_0 t + \omega_{RF} t) \right] \\ & + J_1(\beta_1) J_2(\beta_2) \times \left[\begin{aligned} & \sin(\omega_0 t - 3\omega_{RF} t) + \\ & \sin(\omega_0 t + 3\omega_{RF} t) \end{aligned} \right] \end{aligned} \right\} \quad (21)$$

Considering, $\phi_1 = \phi_2 = 0$ which are the initial phases of the applied RF electrical drive signal of MZM1 and MZM2, respectively and β_1 and β_2 are the modulation depth of the MZM1 and MZM2, respectively. The electric field representing the optical signal at the end of the transmission over an ITU G.653 can be obtained by adding the transmission phase delay $[\beta(\omega_0 \pm 2n\omega_{RF})L]$ to the corresponding optical sideband shown in Eq.(21).

$$E_{out2}(t) = E_0 \left\{ \begin{aligned} & \left[J_1(\beta_1) J_2(\beta_2) - k J_1(\beta_1) J_0(\beta_2) \right] \\ & \times \left[\begin{aligned} & \sin(\omega_0 t - \omega_{RF} t + \beta(\omega_0 - \omega_{RF})L) + \\ & \sin(\omega_0 t + \omega_{RF} t + \beta(\omega_0 + \omega_{RF})L) \end{aligned} \right] \\ & + J_1(\beta_1) J_2(\beta_2) \times \left[\begin{aligned} & \sin(\omega_0 t - 3\omega_{RF} t + \beta(\omega_0 - 3\omega_{RF})L) + \\ & \sin(\omega_0 t + 3\omega_{RF} t + \beta(\omega_0 + 3\omega_{RF})L) \end{aligned} \right] \end{aligned} \right\} \quad (22)$$

Inserting dispersion parameter in Eq.(22) up to fifth order with the help of Eq.(10), Eq.(11), Eq.(12), Eq.(13) and Eq.(14) i.e. the electric field at the output of MZM2 with dispersion is given by,

$$E_{out2}(t) = 2.E_0 \left\{ \begin{aligned} & \left[J_1(\beta_1) J_2(\beta_2) - k J_1(\beta_1) J_0(\beta_2) \right] \\ & \times \sin \left(\begin{aligned} & \omega_0 t + \beta(\omega_0)L + \frac{1}{2} \beta^2(\omega_0)(\omega_{RF})^2 L + \\ & \frac{1}{24} \beta^4(\omega_0)(\omega_{RF})^4 L \end{aligned} \right) \\ & \times \cos \left(\begin{aligned} & \omega_{RF} t + \beta(\omega_0)(4\omega_{RF}L) + \frac{1}{6} \beta^3(\omega_0)(\omega_{RF})^3 L + \\ & \frac{1}{120} \beta^5(\omega_0)(\omega_{RF})^5 L \end{aligned} \right) \\ & + 2.J_1(\beta_1) J_2(\beta_2) \times \sin \left(\begin{aligned} & \omega_0 t + \beta(\omega_0)L + \frac{1}{2} \beta^2(\omega_0)(3\omega_{RF})^2 L + \\ & \frac{1}{24} \beta^4(\omega_0)(3\omega_{RF})^4 L \end{aligned} \right) \\ & \times \cos \left(\begin{aligned} & 3\omega_{RF} t + \beta(\omega_0)(3\omega_{RF}L) + \frac{1}{6} \beta^3(\omega_0)(3\omega_{RF})^3 L + \\ & \frac{1}{120} \beta^5(\omega_0)(3\omega_{RF})^5 L \end{aligned} \right) \end{aligned} \right\}$$

At the end of the fiber, $z = L$, the output intensity of photo detector is given by,

$$I_{PD}(t) = E_{out2} \cdot E_{out2}^* \quad (23)$$

2.4 MAXTP, MINTP

As the MZM1 is biased at the MAXTP and MZM2 is biased at MINTP. Therefore, $\Phi_1 = 0$ and $\Phi_2 = \pi$ for MZM1 and MZM2, respectively. Expanding Eq.(4) for $n = 2$, the electric field ($E_{out1}(t)$) at the output of MZM1 is given by,

$$E_{out1}(t) = E_0 \left\{ \begin{aligned} & J_0(\beta_1) \cos(\omega_0 t) \\ & - J_2(\beta_1) \cos(\omega_0 t - 2\omega_{RF} t - 2\phi_1) \\ & - J_2(\beta_1) \cos(\omega_0 t + 2\omega_{RF} t + 2\phi_1) \end{aligned} \right\} \quad (24)$$

where, ϕ_1 initial phase of an electrical drive is signal for MZM1 and β_1 is the modulation depth of MZM1. If the attenuation of the Fiber Bragg Grating at its center notch wavelength is α dB then the electric field at the output of FBG becomes,

$$E_{out1}(t) = E_0 \left\{ \begin{aligned} & k J_0(\beta_1) \cos(\omega_0 t) \\ & - J_2(\beta_1) \cos(\omega_0 t - 2\omega_{RF} t - 2\phi_1) \\ & - J_2(\beta_1) \cos(\omega_0 t + 2\omega_{RF} t + 2\phi_1) \end{aligned} \right\} \quad (25)$$

where, k is the electrical field attenuation factor and related to α by $\alpha = -20 \log_{10} k$.

As shown in Fig.1, ($E_{out1}(t)$) is input to the second MZM. Therefore, following the similar procedure as done in the above three cases. The electric field ($E_{out2}(t)$) output of MZM2 by considering dispersion parameters up to fifth order is given by,

$$\begin{aligned}
 E_{out2}(t) = & 2.E_0 \{ [J_1(\beta_2).J_2(\beta_1) - J_1(\beta_2).J_0(\beta_2)] \\
 & \times \sin \left(\begin{aligned} & \omega_0 t + \beta(\omega_0)L + \frac{1}{2}\beta^2(\omega_0)(\omega_{RF})^2 L \\ & + \frac{1}{24}\beta^4(\omega_0)(\omega_{RF})^4 L \end{aligned} \right) \\
 & \times \cos \left(\begin{aligned} & \omega_{RF} t + \beta(\omega_0)(4\omega_{RF}L) + \frac{1}{6}\beta^3(\omega_0)(\omega_{RF})^3 L \\ & + \frac{1}{120}\beta^5(\omega_0)(\omega_{RF})^5 L \end{aligned} \right) \\
 & + 2.J_1(\beta_2).J_2(\beta_1) \times \sin \left(\begin{aligned} & \omega_0 t + \beta(\omega_0)L + \frac{1}{2}\beta^2(\omega_0)(3\omega_{RF})^2 L \\ & + \frac{1}{24}\beta^4(\omega_0)(3\omega_{RF})^4 L \end{aligned} \right) \\
 & \times \cos \left(\begin{aligned} & 3\omega_{RF} t + \beta(\omega_0)(3\omega_{RF}L) + \frac{1}{6}\beta^3(\omega_0)(3\omega_{RF})^3 L \\ & + \frac{1}{120}\beta^5(\omega_0)(3\omega_{RF})^5 L \end{aligned} \right)
 \end{aligned}$$

At the end of the fiber, $z = L$, the output intensity of photo detector is given by,

$$I_{PD}(t) = E_{out2} \cdot E_{out2}^* \quad (26)$$

3. RESULTS AND DISCUSSION

In our calculation, we have used the electrical drive signal frequency nearly equal to 12.5 GHz, optical carrier of 193.1THz, modulation depth (β) range of 0 to 2 for both the MZMs and assumed the initial phase of the electrical drive signal for both the MZMs equal to zero. Referring to ITU's G.653 fiber [16]. We have neglected the dispersion parameter $\beta^1(\omega_0) = d\beta/d\omega = \tau$, because it produces only a phase delay of the carrier signal and has no influence on distortion of the microwave signal generation.

$$\text{Fibre chromatic dispersion} = \frac{d\tau}{d\lambda} = D = 4.5 \text{ ps/km nm};$$

$$\text{Dispersion Slope} = \frac{d^2\tau}{d^2\lambda} = D_1 = S = 0.085 \text{ ps/km nm}^2;$$

$$\text{Dispersion curvature} = \frac{d^3\tau}{d^3\lambda} = D_2 = 2.3776 \times 10^{-4} \text{ ps/km nm}^3;$$

$$\text{Dispersion curvature} = \frac{d^4\tau}{d^4\lambda} = D_3 = 7.0647 \times 10^{-6} \text{ ps/km nm}^4 \text{ and}$$

$$\text{Electrical field attenuation factor} = \alpha = 100 \text{ dB.}$$

3.1 MAXTP, MAXTP

In Fig.2, we have shown the combine effect of $\beta^2 + \beta^3 + \beta^4 + \beta^5$ dispersion parameters on the microwave generation using two cascaded MZMs operating in MAXTP- MAXTP condition.

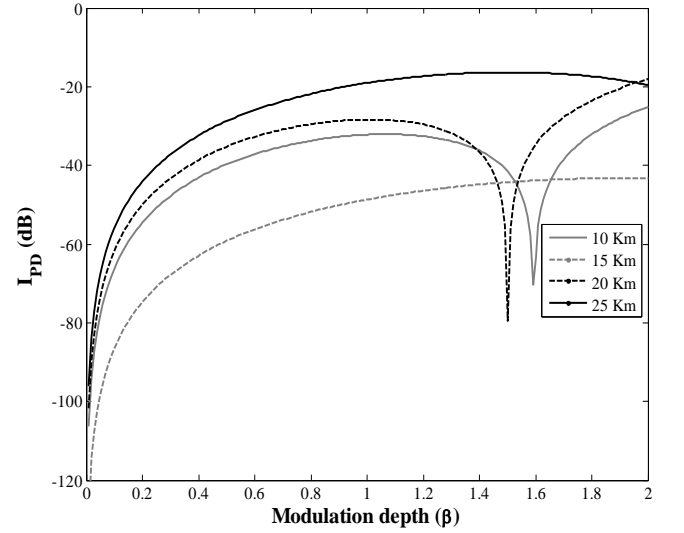


Fig.2. Plot of Intensity (I_{PD}) at the output of Photo Detector versus Modulation depth (β) for the MAXTP, MAXTP at different values of distances under the combined effect of $\beta^2 + \beta^3 + \beta^4 + \beta^5$ MAXTP: Maximum Transmission Point

From Fig.2 we observe that better performance occur for $L = 25$ km and we get two notches at points (1.5, -79.64) and (1.59, -70.27) for $L=10$ km, 20 km, respectively.

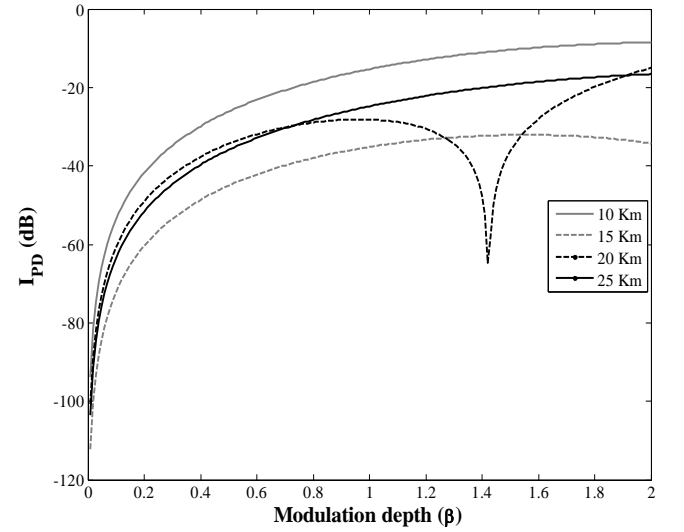


Fig.3. Plot of Intensity (I_{PD}) at the output of Photo Detector versus Modulation depth (β) for the MAXTP, MAXTP at different values of distances under the effect of β^4 only. MAXTP: Maximum Transmission Point

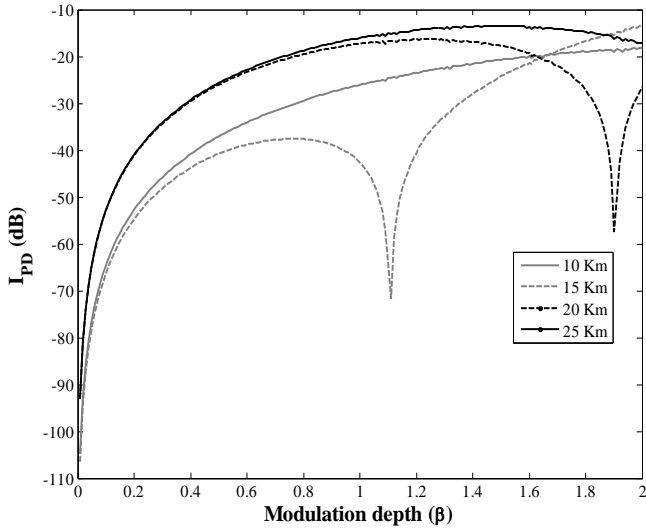


Fig.4. Plot of Intensity (I_{PD}) at the output of Photo Detector versus Modulation depth (β) for the MAXTP, MAXTP at different values of distances under the effect of β^5 only. MAXTP: Maximum Transmission Point

In Fig.3, we plotted the output intensity of photo detector versus modulation depth (β) with due consideration of β^4 dispersion parameter. In this case, at $L = 10$ km better performance occur. Here, the notch occurs at point (1.42, -64.67) for $L = 20$ km. In Fig.4, we plotted the output intensity of photo detector versus modulation depth (β) with consideration of β^5 dispersion parameter. In this case, the better performance take place for $L = 10$ km and $L = 25$ km. Here, we again get two notches at points (1.11, -71.56), (1.9, -57.24) for $L = 15$ km and $L = 20$ km, respectively. Summary of result for different dispersion parameters for MAXTP, MAXTP condition is shown in Table.1. It has been found that the output intensity of photo detector reduces by the combined effect of $\beta^2 + \beta^3 + \beta^4 + \beta^5$ and the dominating dispersion parameter is β^5 .

Table.1. Comparison of Intensity (I_{PD}) At the output of Photo Detector at Different Modulation Index (β) With Combined Effect of Dispersion Parameters for MAXTP, MAXTP Case

Dispersion parameters	Length of Fiber in km	I_{PD} (dB) with $\beta = 1.8$	I_{PD} (dB) with $\beta = 2$
$\beta^2 + \beta^3 + \beta^4 + \beta^5$	10	-32.18	-25.1
	15	-48.68	-43.26
	20	-28.37	-17.95
	25	-19.04	-19.61
β^4 only	10	-15.33	-8.496
	15	-35.15	-34.29
	20	-28.19	-14.99
	25	-24.78	-16.58
β^5 only	10	-26.02	-18.18
	15	-42.58	-13.31
	20	-17.28	-26.57
	25	-16.01	-17.23

3.2 MAXTP, MINTP

The Fig.5 shows the combine effect of $\beta^2 + \beta^3 + \beta^4 + \beta^5$ dispersion parameters on the microwave generation using two cascaded MZMs operating in MAXTP-MINTP condition. Better performance occur at $L = 10$ km. We observed that for $L = 25$ km the response is similar to the Band pass filter and get single notch at point (1.06, -84.55).

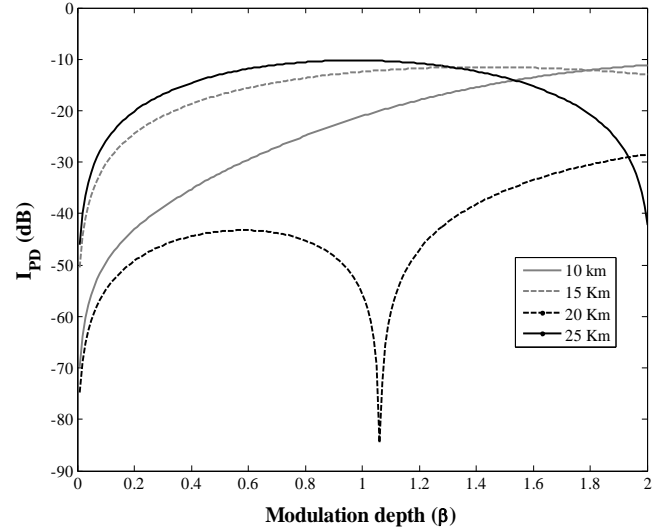


Fig.5. Plot of Intensity (I_{PD}) at the output of Photo Detector versus Modulation depth (β) for the MAXTP, MINTP at different values of distances under the combined effect of $\beta^2 + \beta^3 + \beta^4 + \beta^5$ MAXTP: Maximum Transmission Point, MINTP: Minimum Transmission Point

In Fig.6, we plotted the graph of output photo detector intensity versus modulation depth (β) with due consideration of β^4 term only. Response is similar to the bandpass type response for all fibres. So we can say that fourth order dispersion parameter β^4 alone is dominating dispersion parameter for this case.

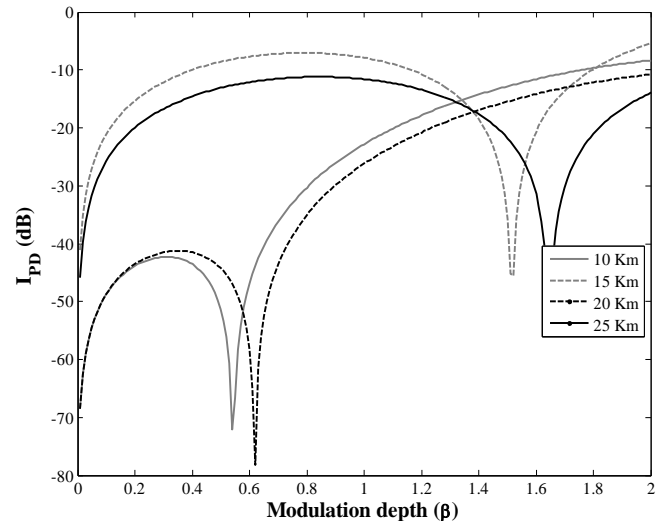


Fig.6. Plot of Intensity (I_{PD}) at the output of Photo Detector versus Modulation depth (β) for the MAXTP, MINTP at different values of distances under the effect of β^4 only. MAXTP: Maximum Transmission Point, MINTP: Minimum Transmission Point

Summary of result for different dispersion parameters for MAXTP, MINTP condition is shown in Table.2.

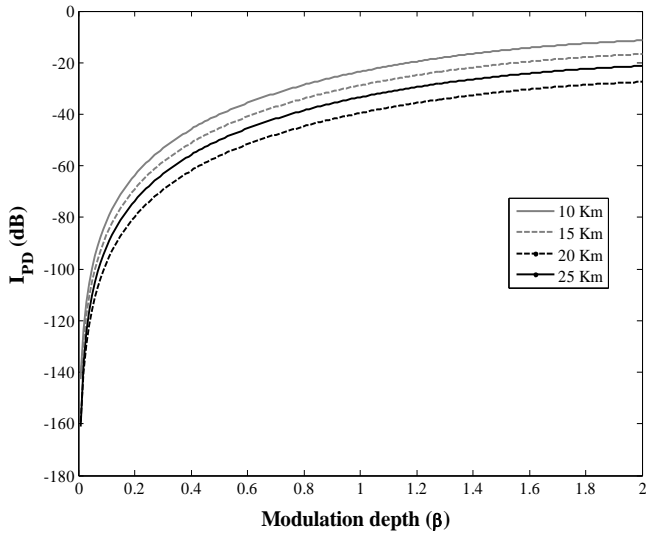


Fig.7. Plot of Intensity (I_{PD}) at the output of Photo Detector versus Modulation depth (β) for the MINTP, MAXTP at different values of distances under the combined effect of $\beta^2 + \beta^3 + \beta^4 + \beta^5$. MAXTP: Maximum Transmission Point, MINTP: Minimum Transmission Point

We observe that the output intensity of photo detector reduces by the combined effect of $\beta^2 + \beta^3 + \beta^4 + \beta^5$ and the dominating dispersion parameter is β^4 .

Table.2. Comparison of Intensity (I_{PD}) at the output of Photo detector at different modulation index (β) with combined effect of dispersion parameters for MAXTP, MINTP case

Dispersion parameters	Length of Fiber in km	I_{PD} (dB) with $\beta = 1.8$	I_{PD} (dB) with $\beta = 2$
$\beta^2 + \beta^3 + \beta^4 + \beta^5$	10	-21.04	-11.12
	15	-12.43	-12.99
	20	-55.56	-28.46
	25	-10.23	-42.24
β^4 only	10	-22.82	-8.342
	15	-7.91	-5.407
	20	-23.2	-10.78
	25	-11.6	-13.95

3.3 MINTP, MAXTP

In Fig.7, we have shown the combine effect of $\beta^2 + \beta^3 + \beta^4 + \beta^5$ dispersion parameters on the microwave generation for MINTP- MAXTP condition. Figure shows that we not get any notch and best response occur at $L = 10$ km. So we can say that dispersion has little effect on microwave generation for MINTP- MAXTP condition. Fig.8 shows the output photo detector intensity versus modulation depth with consideration of β^4 term only. Best response occur for $L = 15$ km and also we observed that no notch occur for this case.

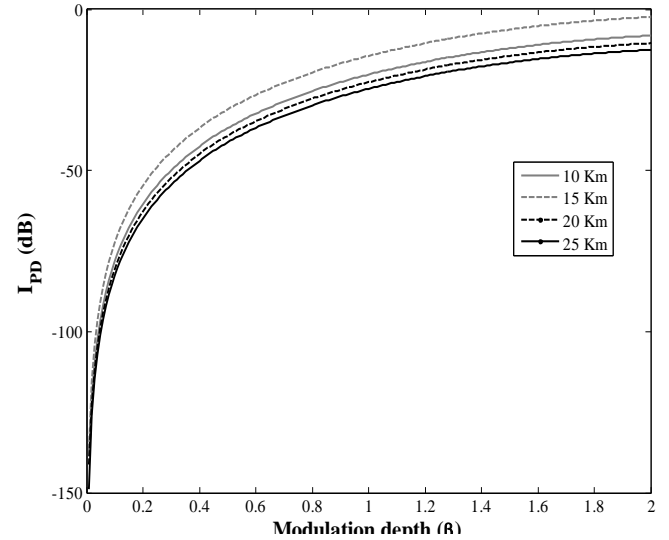


Fig.8. Plot of Intensity (I_{PD}) at the output of Photo Detector versus Modulation depth (β) for the MINTP, MAXTP at different values of distances under the effect of β^4 only. MAXTP: Maximum Transmission Point, MINTP: Minimum Transmission Point

Summary of result for different dispersion parameters for MINTP, MAXTP condition is shown in Table 3. It is found that the output intensity of photo detector reduces by the combined effect of $\beta^2 + \beta^3 + \beta^4 + \beta^5$. From the Figs.(7-8), we can say that dispersion parameter has little effect on microwave generation for the MINTP- MAXTP case.

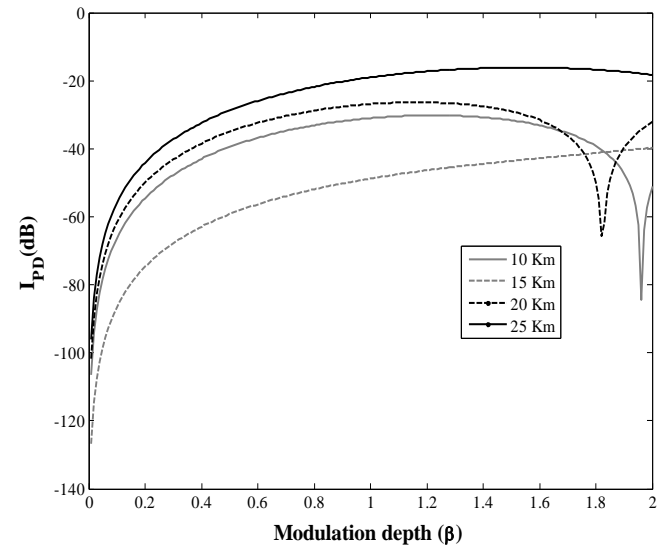


Fig.9. Plot of Intensity (I_{PD}) at the output of Photo Detector versus Modulation depth (β) for the MINTP, MINTP at different values of distances under the combined effect of $\beta^2 + \beta^3 + \beta^4 + \beta^5$. MINTP: Minimum Transmission Point

Table.3. Comparison of Intensity (I_{PD}) at the output of Photo detector at different modulation index (β) with combined effect of dispersion parameters for MINTP, MAXTP case

Dispersion parameters	Length of Fiber in km	I_{PD} (dB) with $\beta = 1.8$	I_{PD} (dB) with $\beta = 2$
$\beta^2 + \beta^3 + \beta^4 + \beta^5$	10	-23.48	-11.39
	15	-28.79	-16.7
	20	-39.54	-27.44
	25	-33.38	-21.28
β^4 only	10	-20.22	-8.126
	15	-14.44	-2.343
	20	-22.59	-10.5
	25	-24.65	-12.56

3.4 MINTP, MINTP

The Fig.9 shows the combine effect of $\beta^2 + \beta^3 + \beta^4 + \beta^5$ dispersion parameters on the microwave generation using two cascaded MZMs operating in MINTP- MINTP condition. We observed that best response occur at $L = 25$ km and found that response resemble to bandpass type response for both fibres ($L=15$ km and $L = 20$ km). Fig.10 shows the plot of output photo detector intensity versus modulation depth (β) with due consideration of β^4 dispersion parameter. Here, better response occur for $L = 10$ km and we observed bandpass type response for both fibre of length $L = 15$ km and 20 km, respectively.

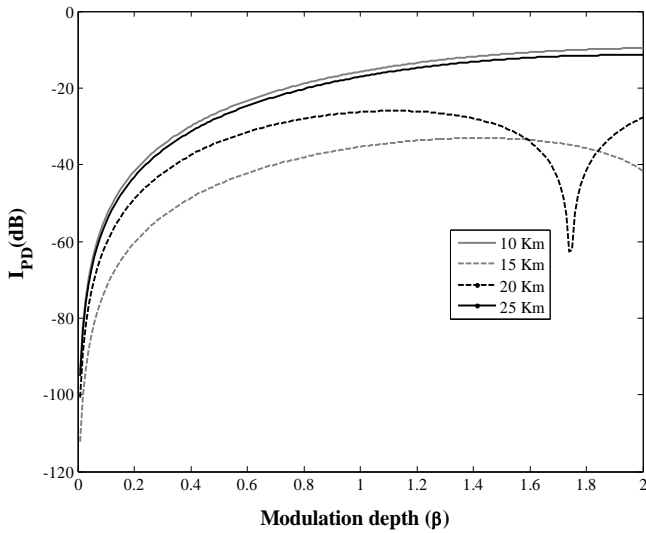


Fig.10. Plot of Intensity (I_{PD}) at the output of Photo Detector versus Modulation depth (β) for the MINTP, MINTP at different values of distances under the effect of β^4 only. MINTP: Minimum Transmission Point

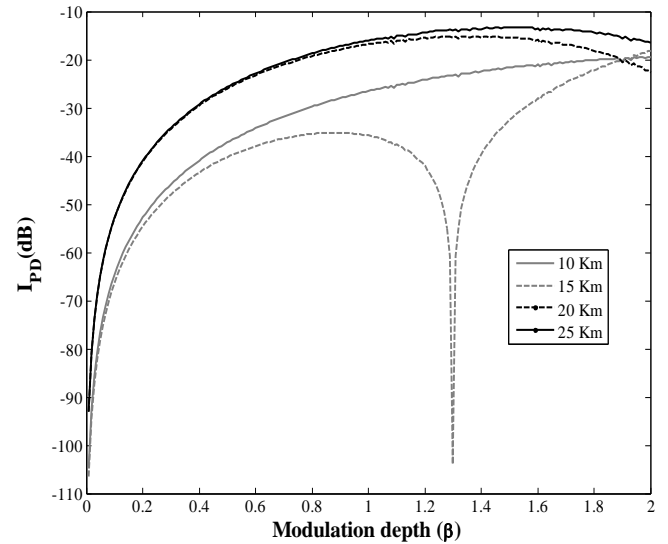


Fig.11. Plot of Intensity (I_{PD}) at the output of Photo Detector versus Modulation depth (β) for the MINTP, MINTP at different values of distances under the effect of β^5 only. MINTP: Minimum Transmission Point

Table.4. Comparison of Intensity (I_{PD}) at the output of Photo detector at different modulation index (β) with combined effect of dispersion parameters for MINTP, MINTP case

Dispersion parameters	Length of Fiber in km	I_{PD} (dB) with $\beta = 1.8$	I_{PD} (dB) with $\beta = 2$
$\beta^2 + \beta^3 + \beta^4 + \beta^5$	10	-31	-51.11
	15	-48.75	-39.7
	20	-26.86	-32.14
	25	-19.02	-18.28
β^4 only	10	-9.59	-15.73
	15	-41.73	-35.33
	20	-27.65	-26.27
	25	-11.47	-17.06
β^5 only	10	-26.51	-19.36
	15	-35.73	-18.09
	20	-16.79	-22.63
	25	-15.98	-16.63

In Fig.11, we try to show that the plot of output photo detector intensity versus modulation depth (β) with due consideration of β^5 dispersion parameter. Here, better response occur for $L = 15$ km only and we observed bandpass type response for case of $L = 15$ km. Summary of result for different dispersion parameters for MINTP, MINTP condition is shown in Table.4. It is found that the output intensity of photo detector reduces by the combined effect of $\beta^2 + \beta^3 + \beta^4 + \beta^5$ and the main dominating dispersion parameter is β^5 .

4. CONCLUSION

In this paper, the detailed theoretical analysis of influence of chromatic dispersion, Dispersion Slope, Dispersion curvature on microwave generation using two cascaded MZMs is discussed. It is observed that higher order dispersion parameters have significant impact on microwave generation. The impact decreases as the order of dispersion term increases. It has been found that dispersion parameter has little effect for the case of MINTP- MAXTP case. We observed that fifth order dispersion parameter is dominating for the case of MAXTP-MAXTP and MINTP-MINTP where as fourth order dispersion term is dominating for the case of MAXTP-MINTP. We notice that effect of dispersion can be reduced by increasing the modulation depth from 1 to 2. According to the theory and simulation in the paper, harmonics at the output of the photo detector is dependent on the frequency and the combined effect of dispersion parameters up to fifth- order dispersion parameter, which is relevant to the fibre length.

ACKNOWLEDGMENT

The authors would like to thanks Ministry of Human Resource Development (MHRD), Govt. of India, New Delhi, for the financial support during project work.

REFERENCES

- [1] A. Seeds, C. H. Lee, E. Funk and Nagamura, "Microwave Guest editorial: Microwave photonics", *Journal of lightwave technology*, Vol. 21, No. 12, pp. 2959 – 2960, 2003.
- [2] A. Seeds, "Microwave photonics", *IEEE Transactions on Microwave Theory and Techniques*, Vol. 50, No. 3, pp. 877 – 887, 2002.
- [3] A. Seeds and K. Williams, "Microwave Photonics," *Journal of Lightwave Technology*, Vol. 24, No. 12, pp. 4628 - 4641, 2006.
- [4] J. P. Yoa, "Microwave photonics," *Journal of Lightwave Technology*, Vol. 27, No. 3, pp. 314 - 335, 2009.
- [5] Jose Capmany and Dalma Novak, "Microwave photonics combines two worlds", *Nature Photonics*, Vol. 1, pp. 319 – 330, 2007.
- [6] S. K. Raghuvanshi and Mandeep Singh, "Effect of Higher Order Dispersion Terms on Microwave Generation Due to Single Mode Fiber, Dispersion Shifted Fiber and Non-Zero Dispersion Shifted Fiber on Lithium Niobate Mach-Zehnder Modulator", *International Journal of Electrical and Electronics Engineering Research*, Vol. 3, No. 1, pp. 189 – 208, 2013.
- [7] Jianping Yao, "A Tutorial on Microwave Photonics", *IEEE Photonics Society Newsletter*, pp. 4 – 12, 2012.
- [8] L. Goldberg, H. F. Taylor, J. F. Weller and D. M. Bloom, "Microwave signal generation with injection-locked laser diodes", *IEEE Electronics Letters*, Vol. 19, No. 13, pp. 491 – 493, 1983.
- [9] T. Jung, J. L. Shen, D. T. K. Tong, S. Murthy, M. C. Wu, T. Tanbun-Ek, W. Wang, R. Lodenkamper, R. Davis, L. J. Lembo and J. C. Brock, "CW Injection Locking of a Mode-Locked Semiconductor Laser as a Local Oscillator Comb for Channelizing Broad-Band RF Signals", *IEEE Transaction on Microwave Theory and Techniques*, Vol. 47, No. 7, pp. 1225 – 1232, 1999.
- [10] M. Hyodo, K. S. Abedin and N. Onodera, "High-Purity, Optoelectronic Millimeter-Wave Signal Generation by Heterodyne Optical Phase-Locking of External-Cavity Semiconductor Lasers", *IEEE Conference on Lasers and Electro-Optics Europe*, 2000.
- [11] T. Ramos and A. J. Seeds, "Fast Heterodyne Optical Phase Lock Loop Using Double Quantum Well Laser Diodes", *IEEE Electronics Letters*, Vol. 28, No. 1, pp. 82 – 83, 1992.
- [12] F. N. Timofeev, S. Bennett, R. Griffin, P. Bayvel, A. J. Seeds, R. Wyatt, R. Kashyap and M. Robertson, "High Spectral Purity Millimeter-Wave Modulated Optical Signal Generation Using Fiber Grating Lasers", *IEEE Electronics Letters*, Vol. 34, No. 7, pp. 668 – 669, 1998.
- [13] J. J. O'Reilly, P. M. Lane, R. Heidemann and R. Hofstetter, "Optical generation of very narrow linewidth millimeter wave signals", *IEEE Electronics Letters*, Vol. 28, No. 25, pp. 2309 – 2311, 1992.
- [14] Wangzhe Li and Jianping Yao, "Investigation of Photonically Assisted Microwave Frequency Multiplication Based on External Modulation", *IEEE Transactions on Microwave Theory and Techniques*, Vol. 58, No. 11, pp. 3259 – 3268, 2010.
- [15] Gerd Keiser, "Optical Fiber Communications", McGraw-Hill, 2010.
- [16] ITU-T Recommendation G.653, "Characteristics of Non Zero Dispersion Shifted Single Mode Optical Fiber Cable", *Series G: Transmission Systems and Media, Digital Systems and Networks*, pp. 1 - 26, 2009.